Phenolic metabolites of anthocyanins modulate mechanisms of endothelial function

Michael Edwards[1], Charles Czank[2], Gary M. Woodward[3], Aedín Cassidy, Colin D. Kay[*]

Department of Nutrition, Norwich Medical School, University of East Anglia, Norwich, U.K., NR4 7TJ

[*]Corresponding author:

Dr Colin D. Kay

Faculty of Medicine and Health Sciences (MED 1 Floor 2), Department of Nutrition, Norwich Medical School, University of East Anglia, Norwich, U.K., NR4 7UQ

Email: Colin.Kay@uea.ac.uk; Telephone: +44 (0)1603 591236

[1] Current address: GFA, Ely, Cambridgeshire, CB7 4EX, UK

[2] Current address: Telethon Kids Institute, University of Western Australia, West Perth, Western Australia

[3] Current address: Department of Clinical Biochemistry, Oxford University Hospitals, Oxford

ABSTRACT

Anthocyanins are reported to have vascular bioactivity, however their mechanisms of action are largely unknown. Evidence suggests that anthocyanins modulate endothelial function, potentially by increasing nitric oxide (NO) synthesis, or enhancing NO bioavailability. This study compared the activity of cyanidin-3-glucoside, its degradation product protocatechuic acid and phase II metabolite, vanillic acid. Production of NO and superoxide, and expression of endothelial NO synthase (eNOS), NADPH oxidase (NOX) and haem oxygenase-1 (HO-1), was established in human vascular cell models. Nitric oxide levels were not modulated by the treatments, although eNOS was upregulated by cyanidin-3-glucoside, and superoxide production was decreased by both phenolic acids. Vanillic acid upregulated $p22^{phox}$ mRNA but did not alter NOX protein expression, although trends were observed for $p47^{phox}$ downregulation and HO-1 upregulation. Anthocyanin metabolites may therefore modulate vascular reactivity by inducing HO-1 and modulating NOX activity, resulting in reduced superoxide production and improved NO bioavailability.

KEYWORDS

Endothelium, eNOS, cyanidin, HUVEC, NADPH oxidase

INTRODUCTION

Epidemiological evidence suggests that higher consumption of anthocyanins, a sub-class of the flavonoid family of polyphenols [1], is inversely associated with risk of hypertension [2] and cardiovascular disease mortality [3, 4]. In recent randomised controlled trials, 12-week consumption of anthocyanins (320 mg/day) was associated with enhanced endothelial function in hypercholesterolaemic individuals [5], while acute consumption (724 mg) elicited a dose-dependent (biphasic) increase in endothelial-dependent vasodilation [6]. Mechanistic studies suggest that anthocyanins may act to enhance vascular function through modulating levels of nitric oxide (NO) [7, 8]. The reduced bioavailability of endothelial-derived NO is critical in the development of atherosclerosis [9]; and a loss of NO in vascular pathologies is mediated by reaction with superoxide anion ($O_2^{\cdot-}$) [10, 11] generated by vascular NADPH oxidase (NOX) enzymes [9, 12] which constitute a major source of reactive oxygen species in the vasculature. Anthocyanins have been reported to elevate the expression of the cytoprotective enzyme haem oxygenase-1 (HO-1) in human vascular endothelial cells [13] and upregulation of HO-1 with subsequent inhibition of NOX activity has been described in cell culture [14] and animal models [15]. Therefore, anthocyanins could potentially improve endothelial function, by increasing the bioavailability of endothelial-derived NO and thus improving vascular homeostasis, by decreasing endothelial NOX activity and $O_2^{\cdot-}$ levels as a result of HO-1 induction.

Anthocyanins are generally reported to have a low relative bioavailability [16, 17], suggesting their bioactivity is mediated by their metabolites, which exist in the systemic circulation at much higher concentrations [17, 18] than their precursor structures. However, most previous studies have explored the activity of anthocyanins *in vitro* as unmetabolised precursor structures, whilst very few have examined the activity of their phenolic metabolites. The aim of the present study was therefore to compare the bioactivity of a parent anthocyanin with its physiologically relevant phenolic acid derivatives, to establish if anthocyanin metabolites share a common or have a differential biological

activity to their unmetabolised structures. Cyanidin-3-glucoside (Figure 1A) was chosen for this study as Czank *et al* (2013) have recently reported the systemic concentrations of its metabolites in humans using an isotope tracer study design [17, 19]. Of the 24 isotope-labelled metabolites identified, the phenolic acid degradation product protocatechuic acid (Figure 1B), and its mono-*O*-methylated metabolite vanillic acid (Figure 1C), were selected for comparison with the parent anthocyanin, as they share structural similarities with the known vasoactive compound apocynin [2].

Bioactivity was assessed by screening physiologically relevant concentrations of the treatments (at 0.1, 1, 10 µM [17]) for effects on eNOS expression and activity, and angiotensin II-stimulated superoxide production, in human umbilical vein endothelial cells (HUVEC). Vanillic acid was ultimately selected to explore mechanisms potentially underlying the observed activity, by examining the modulation of NOX isoforms (and subunits) and HO-1, using both HUVEC and human coronary artery endothelial cells (HCAEC).

MATERIALS AND METHODS

Standards and reagents. Cyanidin-3-glucoside was purchased from Extrasynthese (Genay Cedex, France); VAS2870 from Enzo Life Sciences (Exeter, U.K.); and all other reagents were from Sigma-Aldrich (Poole, U.K.) unless otherwise noted. Stock solutions were prepared in dimethyl sulphoxide (DMSO) and stored at -80°C. Foetal bovine serum (FBS, heat-inactivated) was purchased from Biosera (Ringmer, UK) and tumour necrosis factor-alpha (TNF-α), TRIzol® reagent, and SuperScript® II Reverse Transcriptase were obtained from Life Technologies (Paisley, UK).

Precision 2x real-time PCR MasterMix with SYBR®Green was obtained from PrimerDesign Ltd (Southampton, UK). Custom primer sets for human NOX2, NOX4, $p22^{phox}$, $p47^{phox}$ and $p67^{phox}$

were supplied by PrimerDesign Ltd, and custom primers for human HO-1 (HMOX-1) by Life Technologies. Primer sequences are provided as Supporting Information (Table S1).

NuPAGE sample reducing agent and LDS sample buffer were purchased from Life Technologies, and Precision Plus Protein Dual Colour standards from Bio-Rad Laboratories, Inc (Hemel Hempstead, UK).

Cell culture. Early passage, pooled HUVEC were purchased from TCS Cellworks (Buckingham, UK) and used between passages 2 to 4. Cells were routinely cultured in large vessel endothelial cell growth medium (TCS CellWorks) at 37°C and 5% CO_2. HUVEC were sub-cultured using 0.025% trypsin and 0.01% ethylenediaminetetraacetic acid (EDTA) (TCS CellWorks).

Cryo-preserved, second passage, single donor HCAEC were purchased from PromoCell GmbH (Heidelberg, Germany) and used between passages 3 to 6. Cells were routinely cultured in endothelial cell medium MV (PromoCell GmbH) at 37°C and 5% CO_2. HCAEC were sub-cultured using 0.04% trypsin and 0.03% EDTA (PromoCell GmbH).

Cytotoxicity assay. The maximal level of flavonoids and flavonoid metabolites reported in the systemic circulation is generally below 10 µM [1], hence this concentration was the maximum *in vitro* concentration utilised in the present study. Cell viability following exposure to 10 µM of treatment compounds was determined using cell proliferation reagent WST-1 (Roche Applied Science, Burgess Hill, U.K.) in accordance with the manufacturer's protocol. The assay was conducted using fibronectin-coated microplates seeded with HUVECs at a density of ~10,000 cells/well, and subsequently grown to confluence as determined by light microscopy. After incubation with treatment compounds for 24 h, 10 µl WST-1 reagent was added to each well, and plates were

incubated for a further 4 h. Absorbance was measured at 440 - 450 nm using a microplate reader [Fluostar/Polarstar Optima, BMG Labtech (Aylesbury, U.K.)].

Nitrite/nitrate assay and eNOS enzyme-linked immunosorbent assay (ELISA). Fibronectin-coated 24-well plates were seeded with HUVECs at a density of ~30,000 cells/well, and cells grown to confluence. Cells were then cultured in the absence or presence of treatment compounds (0.1, 1, or 10 µM) for 24 h; after which supernatants were removed and stored at -80°C. Cells were washed once with warm phosphate-buffered saline (PBS), and then harvested in trypsin/EDTA and trypsin-blocking solution. Cell suspensions were stored at -80°C until lysis. Nitric oxide production was assessed using a colourimetric microplate assay (Cayman Chemical Company Nitrate/Nitrite Colourimetric Assay Kit from Cambridge Bioscience, Cambridge, U.K.) according to the manufacturer's instructions. The average intra-assay coefficient of variation (CV) was 6.63% ± 1.10% (mean ± SD, n=3) and the inter-assay CV was 2.38% (n=3). Quantification of eNOS in HUVEC lysates was performed with the Quantikine Human eNOS Immunoassay (R&D Systems, Abingdon, U.K.) according to the manufacturer's instructions. The average intra-assay CV was 4.67% ± 1.86% (mean ± SD, n=3) and the inter-assay CV was 6.10% (n=3).

Stimulated superoxide production assay. Superoxide production was assessed using a modified cytochrome c assay [20, 21]. The modified assay utilised fibronectin-coated 24-well plates seeded with HUVECs at a density of ~50,000 cells/well, and grown to confluence; after which cells were washed once with warm Medium 199 (supplemented with 2% FBS) and incubated for 16-18 h. Cells were then washed once with warm PBS, and incubated for 6 h in supplemented phenol-red free Medium 199 (Invitrogen, Paisley, U.K.) with 0.1 µM angiotensin II, 30 µM ferricytochrome c, and 0.1, 1 or 10 µM of the treatment compounds or 5 µM VAS2870 (selective NOX inhibitor [22]); in the presence or absence of 65 units superoxide dismutase (SOD). Aliquots of cell supernatants were

subsequently transferred to a 96-well microplate for measurement of absorbance at 550 nm. Culture plates were frozen at -80°C for protein extraction.

Direct cytochrome c reduction. Direct reduction of cytochrome c was assessed by co-incubation of treatment compounds in cell-free extracts at concentrations of 2, 20, 200 and 2000 µM with 20 µM cytochrome c in PBS at 37 °C, as described previously for catechols and quinols [23]. The spontaneous reduction of cytochrome c was monitored kinetically at 550 nm over 2 h. Cytochrome c reduction was quantified using the millimolar extinction coefficient for reduced cytochrome c (29.5 $mM.cm^{-1}$).

Superoxide production. Cell-free superoxide production by xanthine/xanthine oxidase was measured using a previously described method [21]. Briefly, 200 µM of cytochrome c, 0.1 U/ml xanthine oxidase and 200 µM xanthine was added to 1, 10, 100 and 1000 µM of the treatment compounds in 50 mM sodium phosphate buffer (pH 7.4). The reaction kinetics of cytochrome c was monitored at 550 nm at 25°C over 15 min (to reaction plateau). Superoxide generated was determined by subtracting the rate of cytochrome c reduction (increase in absorbance at 550 nm) in the presence of SOD versus parallel incubations in the absence of SOD.

Stimulated NOX isoform/subunit gene expression assay. Twenty-four well plates (SPL Life Sciences) coated with fibronectin were seeded with HUVEC at a density of ~30,000 cells/well, and the cells grown to confluence. Culture medium was then aspirated, and the cells were incubated for 16 - 18 h in M199 supplemented with 2% FBS. Thereafter, the cells were incubated for 4 h in supplemented M199 alone (basal), or media with 0.1 µM angiotensin II in the presence or absence of 0.1, 1 or 10 µM vanillic acid. After incubation, the plates were either frozen at -80°C or used for RNA extraction.

Stimulated p47^{phox} protein expression assay. Six-well plates (SPL Life Sciences) coated with fibronectin were seeded with HUVEC or HCAEC at a density of 100,000 cells/well, and cells were grown to confluence. Culture medium was then aspirated, and the cells were incubated for 16 - 18 h in M199 supplemented with 2% FBS (HUVEC only). Cells were subsequently incubated for 5 h in supplemented M199 alone (basal), or media with 20 ng/ml TNF-α in the presence or absence of 0.1, 1, or 10 μM vanillic acid. After incubation, media was aspirated from all wells, and the plates frozen at -80°C until protein extraction.

Endothelial HO-1 expression assay. Expression of HO-1 mRNA/protein was assessed using fibronectin-coated 6-well plates (SPL Life Sciences) seeded with HUVEC or HCAEC at a density of ~100,000 cells/well, and grown to ~70% confluence. Culture medium was then aspirated, and the cells were incubated for 6 h in supplemented culture medium alone (basal), or media with 10 ng/ml phorbol 12-myristate 13-acetate (PMA, positive control), vehicle control (0.005% DMSO; HUVEC only), or 0.1, 1 or 10 μM vanillic acid. After incubation, media was aspirated from all wells and the plates either frozen at -80°C, or used for RNA or protein extraction.

Reverse transcription – quantitative polymerase chain reaction. RNA was extracted from cells using TRIzol® reagent, according to the manufacturer's instructions; and 1 μg of each sample utilised in a reverse transcription reaction with SuperScript® II. Analysis of gene expression was performed using the Applied Biosystems 7500 Real time PCR System (Life Technologies; 7500 software version 2.0) with SYBR®Green detection. Typically, 25 ng of cDNA was amplified with 300 nM of the appropriate primer set. Following enzyme activation at 95°C for 10 minutes, 50 cycles of denaturation (15 seconds at 95°C) and data collection (60 seconds at 60°C) were performed. Relative changes in gene expression were quantified using the comparative C_t method [24]. Optimal stably expressed human reference genes for normalisation of C_t data were identified

using a geNormPLUS kit with primer sets for six genes (PPIA, PRDM4, UBE2D2, UBE4A, TWY1, VIPAS39) supplied by PrimerDesign Ltd.

Immunoblot analysis of endothelial NOX isoform/subunit and HO-1 expression. Cells were harvested and lysed 1% IGEPAL® (octylphenoxy polyethoxyethanol, CA-630), 150 mM NaCl, 20 mM Tris and 10% glycerol (pH 8.0), supplemented with protease inhibitors (Roche Complete Protease Inhibitor Cocktail). Plates were incubated with lysis buffer for 0.5 h at 4°C, and recovered solutions subject to cell disruption by oscillation (50 Hz for 5 minutes with Qiagen TissueLyser LT). After centrifugation at 13,000 rpm (15 minutes at 4°C) the protein content of the supernatants was assayed using the Pierce BCA Protein Assay Kit (Fisher Scientific U.K. Ltd, Loughborough, U.K.) according to manufacturer's instructions.

For SDS-PAGE, cell lysates were reduced using 50 mM dithiothreitol. Briefly, 15 - 25 µg of protein was loaded onto a 4% polyacrylamide stacking gel, and separated across a 10% resolving gel (at 25 mA for 1 h) prior to semi-dry transfer to Immobilon-FL PVDF membrane (Millipore, Watford, UK) at 200 mA for 1.5 h. Membranes were blocked for 1 h at room temperature and incubated overnight (at 4°C) with chicken polyclonal anti-glyceraldehyde-3-phosphate dehydrogenase (GAPDH, Millipore) or goat polyclonal anti-actin (Santa Cruz Biotechnology, Inc., California, U.S.); and either rabbit polyclonal anti-gp91phox (Millipore), rabbit polyclonal anti-NOX4 (Abcam, Cambridge, U.K.), rabbit polyclonal anti-$p47^{phox}$ (Santa Cruz Biotechnology, Inc. or Abcam), or rabbit polyclonal anti-HO-1 (Abcam). Membranes were then washed prior to incubation with either donkey anti-chicken IgG (IR dye 680 LT) or donkey anti-goat IgG (IR dye 680) and goat anti-rabbit IgG (IR dye 800 CW) (Li-Cor, Cambridge, U.K.) for 1 h at room temperature. Membranes were washed and subsequently imaged and quantified using an Odyssey Infrared Imaging System (Li-Cor; Application Software version 3.0.21).

Statistical analysis. Analysis of variance (ANOVA) with LSD post-hoc test was performed using SPSS software (IBM, New York, USA) version 18 for Windows. Significance was determined at the 5% level relative to basal or the assay control. Three biological replicates for each control or treatment were utilised for analysis unless otherwise noted. Means of biological replicates were represented graphically, with error bars denoting standard deviation from the mean. For each control or treatment in the stimulated superoxide production assay, mean absorbance ratio (550 nm/620 nm) in the presence of SOD (n=3) was subtracted from individual absorbance ratio values in the absence of SOD (n=3), to correct for cytochrome c reduction owing to generated superoxide. Mean SOD-corrected absorbance ratio for each treatment was then represented graphically as percentage of that for the angiotensin II control.

RESULTS

Endothelial cytotoxicity. All treatments were screened for cytotoxicity at a concentration of 10 µM; representing the highest concentration used in subsequent bioactivity investigations. No significant effects ($p > 0.05$) on endothelial cell viability were observed following a 24 h incubation of HUVECs with 10 µM of any treatment compound (data not shown).

Endothelial NO production. Cyanidin-3-glucoside, and the phenolic derivatives protocatechuic acid and vanillic acid, did not significantly alter endothelial NO production as measured by levels of NO decomposition products (nitrite & nitrate) in HUVEC supernatants (Supporting Information, Figure S1). Resveratrol (100 µM) and PMA (10 nM) were used as positive controls to confirm the sensitivity of the assay, and elicited significant increases in total nitrite and nitrate (> 270% above basal levels).

eNOS expression in cultured HUVEC. Significant upregulation of eNOS ($p < 0.001$) was observed following 24 h incubation of HUVECs with 0.1, 1 & 10 µM cyanidin-3-glucoside (~4 - 7 fold increase; Figure 2A). No significant alteration in eNOS levels was observed at any concentration of protocatechuic acid (Figure 2B) or vanillic acid (Figure 2C).

Stimulated endothelial superoxide production. The generation of superoxide anion was confirmed using a previously reported NOX inhibitor VAS2870 [22], in the presence and absence of angiotensin II, where co-incubation with VAS2870 significantly reduced superoxide production ($p < 0.01$) (Supporting Information, Figure S2).

Significantly elevated superoxide levels were detected following incubation of cells with 0.1 µM and 1 µM cyanidin-3-glucoside (~3 fold increase; Figure 3A), relative to the angiotensin II-stimulated control. A significant decrease in superoxide ($p < 0.001$) was induced by protocatechuic acid, at 10 µM (~5 fold decrease; Figure 3B), whilst vanillic acid elicited statistically significant reductions ($p < 0.05$) in superoxide at all concentrations examined (~2 fold decrease at 1 µM; Figure 3C). A linear dose-response relationship was not evident for any treatment. Control experiments were conducted to exclude possible confounding through direct reduction of cytochrome c, or scavenging of NOX-derived superoxide radicals, by the treatments. There was no significant impact on cytochrome c reduction (≤ 0.02 nmole.h^{-1}) or superoxide levels (75-106% of control) during incubations with treatment compounds at concentrations up to 10 µM in cell-free systems.

Stimulated endothelial gene expression of NOX isoforms and subunits. Vanillic acid was examined for effects on stimulated endothelial gene expression of the NOX2 and NOX4 isoforms, and the associated subunits $p22^{phox}$, $p47^{phox}$, and $p67^{phox}$. Real time PCR melt curve data indicated non-specific amplification for NOX2, $p47^{phox}$, and $p67^{phox}$ primer sets (data not shown); therefore

relative quantification of gene expression was performed for NOX4 and $p22^{phox}$ only. Co-incubation of HUVEC with angiotensin II and vanillic acid (0.1, 1 and 10 μM) for four hours elicited no significant differences in NOX4 mRNA compared to the angiotensin II control ($p > 0.05$; Figure 4A). A statistically significant ($p < 0.05$) upregulation of $p22^{phox}$ mRNA levels was observed with vanillic acid at 0.1 μM and 1 μM (Figure 4B).

Stimulated endothelial protein expression of NOX isoforms and subunits. The modulation of NOX2 and NOX4 isoforms by vanillic acid was further characterised at the protein level. Following angiotensin II stimulation, weak immunoreactive bands corresponding to NOX2 were visualised by immunoblotting of endothelial lysates, such that quantification of bands by densitometry was not possible (data not shown). By contrast, angiotensin II-induced upregulation of NOX4 expression was observed, although this was not significantly modulated ($p > 0.05$) by co-incubation of cells with angiotensin II and vanillic acid at any concentration examined (0.1-10 μM) (Figure 5).

The effect of vanillic acid on stimulated protein expression of the key NOX2 subunit $p47^{phox}$ was also investigated as a possible mechanism of NOX inhibition. Following co-incubation of HUVEC with 20 ng/ml TNF-α and increasing concentrations of vanillic acid (0.1, 1, or 10 μM) for five hours, a trend towards decreased $p47^{phox}$ expression was observed relative to TNF-α alone (Figure 6A), although these changes were not statistically significant ($p = 0.06$ at 1 μM and 10 μM vanillic acid). A confirmatory experiment was conducted using the HCAEC model, but here no effect was detected on TNF-α stimulated $p47^{phox}$ expression ($p > 0.05$; Figure 6B).

Endothelial HO-1 expression. Modulation of HO-1 expression by vanillic acid was examined as a putative indirect mechanism of NOX inhibition. Incubation of HUVEC with the protein kinase C activator PMA (at 10 ng/ml) for six hours induced a significant increase in basal HO-1 mRNA levels ($p < 0.001$ versus vehicle control; Figure 7). Vanillic acid, at concentrations of 0.1, 1 and 10

μM, elicited a concentration-dependent elevation in endothelial HO-1 mRNA (~1.6-fold versus unstimulated cells with 10 μM vanillic acid), with a trend towards significance compared to vehicle control ($p = 0.1$) at 10 μM (Figure 7). Trends towards elevated expression of HO-1 protein in HUVEC were also observed following a six hour incubation with PMA (~1.9-fold increase versus unstimulated cells) or vanillic acid (~1.8-fold increase at 1 μM vanillic acid) relative to the vehicle control ($p = 0.07$ and $p = 0.1$ respectively; Figure 8A). Since the vehicle control (0.005% DMSO) also appeared to upregulate HO-1 protein, vanillic acid was prepared directly in aqueous solution for use in the HCAEC model, to exclude any vehicle-related effects. Expression of HO-1 protein was slightly elevated following a 6 hour incubation with PMA in the HCAEC model (~1.2-fold increase versus unstimulated cells; Figure 8B). An apparent upregulation of HO-1 protein was observed at all concentrations of vanillic acid tested (Figure 8B), with a trend towards significance at 1 μM (~1.8-fold increase; $p = 0.07$) relative to basal.

DISCUSSION

The low bioavailability of parent anthocyanins suggests their bioactivity *in vivo* is mediated by phenolic metabolites, which have recently been reported as the main circulating species following anthocyanin consumption [17-19]. Here, we report that phenolic metabolites appear to modulate vascular endothelial cell function through alternative mechanisms to those previously described for parent anthocyanins. In the present study, the parent anthocyanin increased eNOS expression, whereas phenolic derivatives had no effect. However, these metabolites elicited reductions in superoxide production, which could subsequently decrease scavenging of NO. Recent studies by Czank *et al* (2013) and de Ferrars *et al* (2014) have confirmed a physiologically appropriate range for anthocyanin metabolites in humans of 0.1 - 10 μM [17-19] and the present study assessed potential mechanisms of activity at these concentrations. Indeed, following consumption of 500 mg ^{13}C-labelled cyanidin-3-glucoside, a serum C_{max} of 1.85 μM has been reported for vanillic acid, with 1

μM concentrations persisting for up to 24 hours [19]; suggesting phenolic derivatives of anthocyanins may be present in the systemic circulation at low micromolar levels for at least 18-24 hours after ingestion of parent anthocyanins. Based on our findings, physiologically relevant levels of anthocyanin metabolites are likely to act indirectly to maintain vascular homeostasis, through induction of HO-1 and decreased endothelial superoxide generation, as opposed to directly stimulating eNOS activity and NO production.

Endothelium-derived nitric oxide is a key component of vascular homeostasis [11] and prior *in vitro* studies have described both upregulation and activation of the eNOS enzyme by anthocyanins (including cyanidin-3-glucoside) in cultured endothelial cells at concentrations ranging from 0.001 μM up to 250 μM [7, 8, 13]. Interestingly, in the present study we observed differential bioactivity for cyanidin-3-glucoside relative to its phenolic acid derivatives. Specifically, no treatment compounds significantly modulated endothelial NO production, however, cyanidin-3-glucoside significantly upregulated eNOS protein levels, while the phenolic derivatives remained inactive (Figure 2).

NOX enzymes represent a major source of reactive oxygen species in the vasculature [12, 25] and anthocyanin metabolites could act as endothelial NOX inhibitors, based on previously reported structure-activity studies [21]. In the current study, differential bioactivity was again observed for cyanidin-3-glucoside relative to its phenolic acid derivatives. A significant elevation in superoxide levels was elicited by cyanidin-3-glucoside; and in contrast, both protocatechuic acid and vanillic acid significantly reduced superoxide levels (Figure 3). Whilst previous reports have described superoxide scavenging [26] and direct cytochrome c reduction [27] elicited by flavonoids, such activity is reported at much higher concentrations (~40 - 100 μM) than those used in the current investigation (≤ 10μM), and control experiments in cell-free incubations confirmed negligible superoxide scavenging or direct cytochrome c reduction by the treatments. High concentrations of phenolic compounds in culture medium have also been reported to result in the generation of

hydrogen peroxide [28], which could potentially interfere with assay methodologies; however, only minimal hydrogen peroxide formation has previously been reported for delphinidin (at 10 µM) [28] which is one of the most reactive anthocyanins [29]. Therefore, data from cell-free experiments in the current study indicate that the treatment compounds do not directly scavenge superoxide radicals, as negligible activity was observed, and the present findings likely reflect reduced endothelial superoxide generation as opposed to radical scavenging.

The phenolic derivative vanillic acid (the methylated metabolite of protocatechuic acid) was subsequently selected to explore mechanisms potentially underlying the observed reductions in superoxide production. In the present study, vanillic acid at a concentration of 1 µM significantly reduced endothelial superoxide levels, which is comparable to the C_{max} value reported by Czank *et al* (2013) for ^{13}C-labelled phase II conjugates of protocatechuic acid (2.35 µM) following ingestion of ^{13}C-labelled cyanidin-3-glucoside [17]. Steffen *et al* (2008) have previously described NOX inhibitory activity of vanillic acid in disintegrated HUVEC (IC_{50} = 8.1 µM), with minimal direct superoxide scavenging activity in a cell-free system (IC_{50} > 100 µM) [21]; which was confirmed by the absence of direct superoxide scavenging by vanillic acid in the present study.

NOX4 is reported to be the major vascular endothelial isoform [30, 31], producing mainly hydrogen peroxide [32]; and whilst NOX4-derived hydrogen peroxide would not act to limit NO bioavailability [33], it might induce vasodilation through hyperpolarisation independently of NO activity [34]. In contrast NOX2 generates superoxide [35] and may have a key role in regulating vascular function [32, 36]. Both NOX2 and NOX4 associate with the integral membrane protein $p22^{phox}$ [37], but activation of NOX2 follows the recruitment of additional cytosolic proteins including $p47^{phox}$ ('organiser' subunit) and $p67^{phox}$ ('activator' subunit) [37, 38]. Modulation of the expression of NOX2 and NOX4 isoforms, and associated subunits ($p22^{phox}$, $p47^{phox}$, and $p67^{phox}$) by vanillic acid was therefore explored using RT-qPCR. Co-incubation of angiotensin II with vanillic acid elicited no significant

changes in levels of endothelial NOX4 mRNA relative to angiotensin II alone (Figure 4A). However, a significant upregulation of $p22^{phox}$ mRNA levels was observed with 0.1 and 1 μM vanillic acid (Figure 4B), whilst we were unable to assess transcriptional modulation of the superoxide-generating NOX2 isoform, or $p47^{phox}$ and $p67^{phox}$. Therefore the effects of vanillic acid on the stimulated expression of NOX2 and $p47^{phox}$, and also NOX4, were explored at the protein level.

There was no significant modulation of stimulated NOX4 protein expression by vanillic acid (Figure 5), indicating that this particular metabolite does not affect endothelial NOX4 protein. NOX2 expression was more difficult to discern by immunoblotting of cell lysates, which may reflect low mRNA/protein expression in vascular cells, and/or poor antibody specificity; although upregulation of NOX2 in HUVECs following angiotensin II stimulation has been previously reported [20]. Interestingly, the observed elevation in $p22^{phox}$ mRNA induced by vanillic acid did not appear to be associated with increased NOX4 or NOX2 protein levels. Modulation of $p47^{phox}$ protein expression was examined as a possible mechanism of NOX2 inhibition, and here a trend was observed towards downregulation of $p47^{phox}$ protein following co-incubation with TNF-α and vanillic acid (Figure 6A). Interestingly, in the HCAEC model, vanillic acid did not modulate stimulated $p47^{phox}$ expression (Figure 6B), and thus vanillic acid does not appear to significantly alter $p47^{phox}$ levels (under the present conditions) and therefore affect NOX2 activity by this mechanism. However, the anthocyanidin delphinidin has recently been reported to inhibit $p47^{phox}$ translocation and NOX activity in human dermal fibroblasts [39], suggesting another potential mechanism by which anthocyanins and/or their degradation products could modulate NOX function.

Upregulation of HO-1 has been reported to inhibit NOX function [14, 15]; and previous studies have described induction of HO-1 expression by anthocyanins and/or their metabolites in human

endothelial cells [13, 40]. For example, Nrf2 nuclear translocation and HO-1 expression in cultured HUVEC was elicited by serum samples obtained from healthy subjects following ingestion of 160 mg purified anthocyanins, which may reflect activity of anthocyanin metabolites as opposed to parent compounds [40]. Moreover, delphindin-3-glucoside has previously been reported to enhance survival of murine hepatocytes exposed to a cytotoxic concentration of epigallocatechin-3-gallate through upregulation of HO-1 mRNA levels [41]. Endothelial homeostasis is maintained through the action of vasodilators such as NO, however NO bioactivity is diminished by radicals such as $O_2^{\cdot -}$ which are produced through activation of NOX [9, 12]. Anthocyanin metabolites could potentially indirectly maintain vascular homeostasis by inducing HO-1, with subsequent inhibition of NOX activity, thus reducing the scavenging of NO by NOX-derived superoxide [14, 15, 40]. Therefore the potential indirect effect of vanillic acid on NOX activity was explored by assessing modulation of endothelial HO-1 expression. Following exposure of HUVEC to vanillic acid, elevated HO-1 mRNA levels were observed in what appeared to be a concentration-dependent response (Figure 7), with a trend towards significance relative to the vehicle control (at 10 µM vanillic acid). Likewise, vanillic acid increased HUVEC HO-1 protein expression (Figure 8A), and densitometric analysis indicated a trend towards significance at 1 µM. The vehicle control also appeared to moderately upregulate HO-1, reflecting previously reported studies in HUVEC with low concentrations of DMSO (0 - 0.8%) [42]. As such, vanillic acid was prepared directly in aqueous solution for investigation in the HCAEC model; where a similar trend for upregulation of HO-1 protein was evident (at 1 µM; Figure 8B), suggesting an inverted U-shaped dose-response.

A possible limitation of the current investigation was the use of HUVEC as an *in vitro* model. Whilst HUVEC are widely used for research concerning general properties of endothelial cells [43], an arterial endothelial cell type may be more appropriate for studies investigating the potential modulation of NOX activity in relation to endothelial dysfunction. Thus as part of the current investigation confirmatory studies were conducted for potential modulation of $p47^{phox}$/HO-1

expression, using HCAEC as a more physiologically representative endothelial model. Furthermore, in the present study there was no effect of cyanidin-3-glucoside on endothelial NO production (Supporting Information, Figure S1), despite a previous report of activation of eNOS by cyanidin-3-glucoside at concentrations of ≤5 μM in HUVECs [7]. It is possible that assessing eNOS activity by investigating enzyme phosphorylation, as described previously for blackcurrant anthocyanins in a HUVEC model [44], could have provided further information as to the effects of treatment compounds upon eNOS. NO production was clearly increased by PMA and resveratrol in control experiments, indicating adequate assay sensitivity for the detection of NO-derived nitrite/nitrate in aqueous solution. It is however possible that the assay was not sensitive enough to detect subtle changes in nitrite/nitrate. Interestingly, and with the possible exception of the upregulation of eNOS by cyanidin-3-glucoside, linear dose-response relationships were not observed for any treatment in the current investigation, suggesting differential bioactivity of anthocyanins and their metabolites across dose ranges, as described previously for cyanidin-3-glucoside [8]. However, as only three concentrations of the treatment compounds were assessed in the current study, it is not possible to draw definitive conclusions regarding dose-response relationships, and a wider dosage range is required to confirm our observations.

Another limitation of the present study was the poor qPCR specificity observed for NOX2, $p47^{phox}$ and $p67^{phox}$, which precluded determination of relative changes in expression for these transcripts. Previously reported studies have suggested low or no endothelial expression of NOX2 mRNA [30, 45], and low expression of $p47^{phox}$ and $p67^{phox}$ mRNA in HUVEC [30]. Moreover, minimal changes were detected in NOX4 gene expression, and $p47^{phox}$ protein expression, following stimulation with angiotensin II or TNF-α respectively; although limited upregulation of $p47^{phox}$ was consistent in both HUVEC and HCAEC models.

In the present study, cyanidin-3-glucoside significantly upregulated endothelial expression of eNOS as previously reported for unmetabolised anthocyanins [8, 13], however the phenolic acid derivatives were not active. By contrast, both the degradation product protocatechuic acid, and its phase II metabolite vanillic acid, significantly reduced endothelial superoxide levels; whereas the parent anthocyanin did not. These data suggest a differential bioactivity of anthocyanins relative to their phenolic derivatives. Our findings therefore indicate that anthocyanins may directly stimulate eNOS, eliciting improved endothelial function; however, when anthocyanins are metabolized, this direct effect upon eNOS is lost. Nevertheless, their metabolites could maintain vascular homeostasis through indirectly preserving NO bioactivity, by mechanisms involving NOX or HO-1. It must be noted that Czank *et al* (2013) identified 16 phenolic metabolites of cyanidin-3-glucoside in human serum [17], which should all be investigated for potential vascular bioactivity in future studies. Indeed, preliminary data from ongoing studies in our laboratory suggest PCA, and PCA in combination with VA, upregulate HO-1 protein expression in rat aortic smooth muscle cells *in vitro* (data not shown).

In conclusion, there was no direct effect of vanillic acid on endothelial protein expression of eNOS or NOX isoforms in the present investigation, whereas HO-1 protein was modestly increased; indicating different mechanisms of bioactivity for phenolic derivatives relative to parent anthocyanins. This also suggests a potential indirect activity of anthocyanin metabolites in maintaining vascular homeostasis *in vivo*.

ABBREVIATIONS USED

Ang II, angiotensin II; ANOVA, analysis of variance; CV, coefficient of variation; DMSO, dimethyl sulphoxide; EDTA, ethylenediaminetetraacetic acid; ELISA, enzyme-linked immunosorbent assay; eNOS, endothelial nitric oxide synthase; FBS; foetal bovine serum; GAPDH, glyceraldehyde-3-phosphate dehydrogenase; HCAEC, human coronary artery endothelial cell; HO-1, haem oxygenase-1; HUVEC, human umbilical vein endothelial cell; NADPH, reduced nicotinamide adenine dinucleotide phosphate; NO, nitric oxide; NOX, NADPH oxidase; $O_2^{\cdot -}$, superoxide; PBS, phosphate-buffered saline; PMA, phorbol 12-myristate 13-acetate; SOD, superoxide dismutase; TNF-α, tumour necrosis factor-alpha; VA, vanillic acid.

ACKNOWLEDGEMENTS

This study was supported by a two UK Biotechnology and Biological Sciences Research Council (BBSRC) CASE studentships (M. Edwards & Gary Woodward) in partnership with GlaxoSmithKline (UK).The authors would like to thank Ilde Rodriguez-Ramiro and Emily Warner (Department of Nutrition, Norwich Medical School, University of East Anglia) for their work on the bioactivity of flavonoids and phenolic metabolites in rat aortic smooth muscle cells (supported by the BBSRC Diet and Health Research Industry Club; BB/H004963/1, BB/I006028/1,).

The authors have declared no conflict of interest.

SUPPORTING INFORMATION DESCRIPTION

Primer sequences for custom primer sets (human HMOX-1, NOX2, NOX4, $p22^{phox}$, $p47^{phox}$ and $p67^{phox}$) are provided as Supporting Information.

REFERENCES

1. Crozier A., Jaganath I. B.; Clifford M. N. Dietary phenolics: chemistry, bioavailability and effects on health. *Nat. Prod. Rep.* **2009**, *26*, 1001-43.

2. Cassidy A., O'Reilly E. J., Kay C., Sampson L., Franz M., Forman J., Curhan G.; Rimm E. B. Habitual intake of flavonoid subclasses and incident hypertension in adults. *Am. J Clin. Nutr.* **2010**, *93*, 338-47.

3. Mink P. J., Scrafford C. G., Barraj L. M., Harnack L., Hong C. P., Nettleton J. A.; Jacobs D. R., Jr. Flavonoid intake and cardiovascular disease mortality: a prospective study in postmenopausal women. *Am. J Clin. Nutr.* **2007**, *85*, 895-909.

4. McCullough M. L., Peterson J. J., Patel R., Jacques P. F., Shah R.; Dwyer J. T. Flavonoid intake and cardiovascular disease mortality in a prospective cohort of US adults. *Am. J Clin. Nutr.* **2012**, *95*, 454-64.

5. Zhu Y., Xia M., Yang Y., Liu F., Li Z., Hao Y., Mi M., Jin T.; Ling W. Purified Anthocyanin Supplementation Improves Endothelial Function via NO-cGMP Activation in Hypercholesterolemic Individuals. *Clin. Chem.* **2011**, *57*, 1524-33.

6. Rodriguez-Mateos A., Rendeiro C., Bergillos-Meca T., Tabatabaee S., George T. W., Heiss C.; Spencer J. P. Intake and time dependence of blueberry flavonoid–induced improvements in vascular function: a randomized, controlled, double-blind, crossover intervention study with mechanistic insights into biological activity. *Am. J Clin. Nutr.* **2013**, *98*, 1179-91.

7. Xu J. W., Ikeda K.; Yamori Y. Cyanidin-3-glucoside regulates phosphorylation of endothelial nitric oxide synthase. *FEBS Lett.* **2004**, *574*, 176-80.

8. Xu J. W., Ikeda K.; Yamori Y. Upregulation of endothelial nitric oxide synthase by cyanidin-3-glucoside, a typical anthocyanin pigment. *Hypertension*. **2004**, *44*, 217-22.

9. Higashi Y., Noma K., Yoshizumi M.; Kihara Y. Endothelial function and oxidative stress in cardiovascular diseases. *Circ. J*. **2009**, *73*, 411-8.

10. Wever R., Stroes E.; Rabelink T. J. Nitric oxide and hypercholesterolemia: a matter of oxidation and reduction? *Atherosclerosis*. **1998**, *137 Suppl*, S51-60.

11. Naseem K. M. The role of nitric oxide in cardiovascular diseases. *Mol. Aspects Med.* **2005**, *26*, 33-65.

12. Bonomini F., Tengattini S., Fabiano A., Bianchi R.; Rezzani R. Atherosclerosis and oxidative stress. *Histol. Histopathol.* **2008**, *23*, 381-90.

13. Sorrenti V., Mazza F., Campisi A., Di Giacomo C., Acquaviva R., Vanella L.; Galvano F. Heme oxygenase induction by cyanidin-3-O-beta-glucoside in cultured human endothelial cells. *Mol. Nutr. Food Res.* **2007**, *51*, 580-6.

14. Jiang F., Roberts S. J., Datla S.; Dusting G. J. NO modulates NADPH oxidase function via heme oxygenase-1 in human endothelial cells. *Hypertension*. **2006**, *48*, 950-7.

15. Datla S. R., Dusting G. J., Mori T. A., Taylor C. J., Croft K. D.; Jiang F. Induction of Heme Oxygenase-1 In Vivo Suppresses NADPH Oxidase–Derived Oxidative Stress. *Hypertension*. **2007**, *50*, 636-42.

16. Vitaglione P., Donnarumma G., Napolitano A., Galvano F., Gallo A., Scalfi L.; Fogliano V. Protocatechuic acid is the major human metabolite of cyanidin-glucosides. *J Nutr.* **2007**, *137*, 2043-8.

17. Czank C., Cassidy A., Zhang Q., Morrison D. J., Preston T., Kroon P. A., Botting N. P.; Kay C. D. Human metabolism and elimination of the anthocyanin, cyanidin-3-glucoside: a ^{13}C-tracer study. *Am. J Clin. Nutr.* **2013**, *97*, 995-1003.

18. de Ferrars R. M., Cassidy A., Curtis P.; Kay C. D. Phenolic metabolites of anthocyanins following a dietary intervention study in post-menopausal women. *Mol. Nutr. Food Res.* **2014**, *58*, 490-502.

19. de Ferrars R. M., Czank C., Zhang Q., Botting N. P., Kroon P. A., Cassidy A.; Kay C. D. The pharmacokinetics of anthocyanins and their metabolites in humans. *Br. J Pharmacol.* **2014**, *171*, 3268-82.

20. Rueckschloss U., Quinn M. T., Holtz J.; Morawietz H. Dose-dependent regulation of NAD(P)H oxidase expression by angiotensin II in human endothelial cells: protective effect of angiotensin II type 1 receptor blockade in patients with coronary artery disease. *Arterioscler. Thromb. Vasc. Biol.* **2002**, *22*, 1845-51.

21. Steffen Y., Gruber C., Schewe T.; Sies H. Mono-O-methylated flavanols and other flavonoids as inhibitors of endothelial NADPH oxidase. *Arch. Biochem. Biophys.* **2008**, *469*, 209-19.

22. Stielow C., Catar R. A., Muller G., Wingler K., Scheurer P., Schmidt H. H.; Morawietz H. Novel Nox inhibitor of oxLDL-induced reactive oxygen species formation in human endothelial cells. *Biochem. Biophys. Res. Commun.* **2006**, *344*, 200-5.

23. Saleem M. M.; Wilson M. T. Kinetic studies on the reduction of cytochrome c. Reaction with dihydroxy conjugated compounds (catechols and quinols). *Biochem J.* **1982**, *201*, 433-44.

24. Schmittgen T. D.; Livak K. J. Analyzing real-time PCR data by the comparative C(T) method. *Nat. Protoc.* **2008**, *3*, 1101-8.

25. Bedard K.; Krause K. H. The NOX family of ROS-generating NADPH oxidases: physiology and pathophysiology. *Physiol. Rev.* **2007**, *87*, 245-313.

26. Taubert D., Breitenbach T., Lazar A., Censarek P., Harlfinger S., Berkels R., Klaus W.; Roesen R. Reaction rate constants of superoxide scavenging by plant antioxidants. *Free Rad. Biol. Med.* **2003**, *35*, 1599-607.

27. Skemiene K., Rakauskaite G., Trumbeckaite S., Liobikas J., Brown G. C.; Borutaite V. Anthocyanins block ischaemia-induced apoptosis in the perfused heart and support mitochondrial respiration potentially by reducing cytosolic cytochrome c. *Int. J Biochem. Cell. Biol.* **2012**, *45*, 23-9.

28. Long L. H., Hoi A.; Halliwell B. Instability of, and generation of hydrogen peroxide by, phenolic compounds in cell culture media. *Arch. Biochem. Biophys.* **2010**, *501*, 162-9.

29. Woodward G., Kroon P., Cassidy A.; Kay C. Anthocyanin stability and recovery: implications for the analysis of clinical and experimental samples. *J Agric. Food Chem.* **2009**, *57*, 5271-8.

30. Ago T., Kitazono T., Ooboshi H., Iyama T., Han Y. H., Takada J., Wakisaka M., Ibayashi S., Utsumi H.; Iida M. Nox4 as the Major Catalytic Component of an Endothelial NAD(P)H Oxidase. *Circulation*. **2004**, *109*, 227-33.

31. Takac I., Schroder K.; Brandes R. P. The Nox Family of NADPH Oxidases: Friend or Foe of the Vascular System? *Curr. Hypertens. Rep.* **2011**, *14*, 70-8.

32. Brown D. I.; Griendling K. K. Nox proteins in signal transduction. *Free Radic. Biol. Med.* **2009**, *47*, 1239-53.

33. Brandes R. P., Takac I.; Schroder K. No Superoxide--No Stress?: Nox4, the Good NADPH Oxidase! *Arterioscler. Thromb. Vasc. Biol.* **2011**, *31*, 1255-7.

34. Ray R., Murdoch C. E., Wang M., Santos C. X., Zhang M., Alom-Ruiz S., Anilkumar N., Ouattara A., Cave A. C., Walker S. J., Grieve D. J., Charles R. L., Eaton P., Brewer A. C.; Shah A. M. Endothelial Nox4 NADPH Oxidase Enhances Vasodilatation and Reduces Blood Pressure In Vivo. *Arterioscler. Thromb. Vasc. Biol.* **2011**, *31*, 1368-76.

35. Brandes R. P., Weissmann N.; Schroder K. NADPH oxidases in cardiovascular disease. *Free Radic. Biol. Med.* **2010**, *49*, 687-706.

36. Schroder K. Isoform specific functions of Nox protein-derived reactive oxygen species in the vasculature. *Curr. Opin. Pharmacol.* **2010**, *10*, 122-6.

37. Sumimoto H., Miyano K.; Takeya R. Molecular composition and regulation of the Nox family NAD(P)H oxidases. *Biochem. Biophys. Res. Commun.* **2005**, *338*, 677-86.

38. Drummond G. R., Selemidis S., Griendling K. K.; Sobey C. G. Combating oxidative stress in vascular disease: NADPH oxidases as therapeutic targets. *Nat. Rev. Drug Discov.* **2011**, *10*, 453-71.

39. Lim T.-G., Jung S. K., Kim J.-e., Kim Y., Lee H. J., Jang T. S.; Lee K. W. NADPH oxidase is a novel target of delphinidin for the inhibition of UVB-induced MMP-1 expression in human dermal fibroblasts. *Exp. Dermatol.* **2013**, *22*, 428-30.

598 40. Cimino F., Speciale A., Anwar S., Canali R., Ricciardi E., Virgili F., Trombetta D.; Saija A.
599 Anthocyanins protect human endothelial cells from mild hyperoxia damage through modulation of
600 Nrf2 pathway. *Genes Nutr.* **2013**, *8*, 391-9.
601 41. Inoue H., Maeda-Yamamoto M., Nesumi A.; Murakami A. Delphinidin-3-O-galactoside
602 protects mouse hepatocytes from (-)-epigallocatechin-3-gallate-induced cytotoxicity via up-
603 regulation of heme oxygenase-1 and heat shock protein 70. *Nutr. Res.* **2012**, *32*, 357-64.
604 42. Liang C., Xue Z., Cang J., Wang H.; Li P. Dimethyl sulfoxide induces heme oxygenase-1
605 expression via JNKs and Nrf2 pathways in human umbilical vein endothelial cells. *Mol. Cell*
606 *Biochem.* **2011**, *355*, 109-15.
607 43. Baudin B., Bruneel A., Bosselut N.; Vaubourdolle M. A protocol for isolation and culture of
608 human umbilical vein endothelial cells. *Nat. Protoc.* **2007**, *2*, 481-5.
609 44. Edirisinghe I., Banaszewski K., Cappozzo J., McCarthy D.; Burton-Freeman B. M. Effect of
610 Black Currant Anthocyanins on the Activation of Endothelial Nitric Oxide Synthase (eNOS) in
611 Vitro in Human Endothelial Cells. *J Agric. Food Chem.* **2011**, *59*, 8616–24.
612 45. Alvarez E., Rodino-Janeiro B. K., Ucieda-Somoza R.; Gonzalez-Juanatey J. R. Pravastatin
613 counteracts angiotensin II-induced upregulation and activation of NADPH oxidase at plasma
614 membrane of human endothelial cells. *J Cardiovasc. Pharmacol.* **2010**, *55*, 203-12.

615

616

FIGURE CAPTIONS

Figure 1. Chemical structures of the anthocyanin cyanidin-3-glucoside (A), its B-ring degradation product protocatechuic acid (B), and the mono-*O*-methylated metabolite of protocatechuic acid, vanillic acid (C). COMT, catechol-O-methyltransferase.

Figure 2. Modulation of endothelial eNOS expression (as quantified by ELISA of cell lysates) following 24 h incubation of HUVECs with vehicle control [0.05% DMSO in supplemented culture medium] (VC), or 0.1-10 µM of cyanidin-3-glucoside (A), protocatechuic acid (B), and vanillic acid (C). Data are graphed as mean eNOS protein as percentage of vehicle control (designated as 100% and marked by dashed line); mean ± SD (n=3). *Significant difference versus vehicle control ($p < 0.05$).

Figure 3. Modulation of angiotensin II (Ang II)-stimulated HUVEC endothelial superoxide production by 0.1-10 µM cyanidin-3-glucoside (A), protocatechuic acid (B), or vanillic acid (C). Superoxide production was quantified by reduction of extracellular ferricytochrome c. Data are graphed as SOD-corrected mean absorbance (OD) ratio (550 nm/620 nm) as percentage of Ang II control (designated as 100% and marked by dashed line); mean ± SD (n=3). *Significant difference versus Ang II-stimulated control ($p < 0.05$).

Figure 4. Modulation of HUVEC NOX4 (A) or $p22^{phox}$ (B) mRNA levels following 4 h incubation with 0.1 µM angiotensin II control (Ang II), or Ang II with 0.1 µM, 1 µM or 10 µM vanillic acid, presented as fold change versus unstimulated cells (basal; designated as 1 and marked by dashed line). Relative quantification was performed by RT-qPCR using the comparative C_t method, incorporating the geometric mean of reference genes UBE4A and VIPAS39 as the normalisation

642 factor. Data are graphed as mean ± SD (n=3). *Significant difference versus Ang II-stimulated
643 control ($p < 0.05$).
644
645 **Figure 5**. Expression of NOX4 protein in cell lysates from unstimulated HUVECs (basal) and
646 following 6 h incubation with 0.1 µM angiotensin II (Ang II), or Ang II with 0.1 µM, 1 µM or 10
647 µM vanillic acid (VA). Glyceraldehyde-3-phosphate dehydrogenase (GAPDH) was utilised as a
648 loading control for immunoblotting of cell lysates. Graphs show fold increase in NOX4 expression
649 relative to basal (designated as 1 and marked by dashed line), after quantification by densitometry
650 and normalisation to loading control (mean ± SD, n=5).
651
652 **Figure 6.** Expression of $p47^{phox}$ protein in HUVEC (A) or HCAEC (B) lysates from unstimulated
653 cells (basal) and following 5 h incubation with 20ng/ml TNF-α, or TNF-α with 0.1 µM, 1 µM or 10
654 µM vanillic acid. Glyceraldehyde-3-phosphate dehydrogenase (GAPDH) was utilised as a loading
655 control for immunoblotting of cell lysates. Graphs show fold increase in $p47^{phox}$ expression relative
656 to basal (designated as 1 and marked by dashed line), after quantification by densitometry and
657 normalisation to loading control. Data are graphed as mean ± SD (n=5 for HUVEC and n=4 for
658 HCAEC).
659
660 **Figure 7.** Modulation of HUVEC HO-1 mRNA levels following 6 h incubation with vehicle control
661 (VC, 0.005% DMSO), 10 ng/ml phorbol 12-myristate 13-acetate (PMA), or 0.1 µM, 1 µM or 10
662 µM vanillic acid, presented as fold change versus untreated (basal) cells (designated as 1 and
663 marked by dashed line). Relative quantification was performed by RT-qPCR using the comparative
664 C_t method, incorporating the geometric mean of human reference genes TYW1 and PPIA as the
665 normalisation factor. Data are graphed as mean ± SD (n=3). *Significant difference versus vehicle
666 control (*$p < 0.01$).
667

668 **Figure 8.** Expression of HO-1 protein in HUVEC (A) or HCAEC (B) lysates from untreated cells
669 (basal) and following 6 h incubation with 10 ng/ml phorbol 12-myristate 13-acetate (PMA), vehicle
670 control (VC, 0.005% DMSO; HUVEC only) or 0.1 μM, 1 μM or 10 μM vanillic acid.
671 Glyceraldehyde-3-phosphate dehydrogenase (GAPDH) was utilised as a loading control for
672 immunoblotting of cell lysates. Graphs show fold increase in HO-1 expression relative to basal
673 (designated as 1 and marked by dashed line), after quantification by densitometry and normalisation
674 to loading control. Data are graphed as mean ± SD (n=4).
675

Figure 1

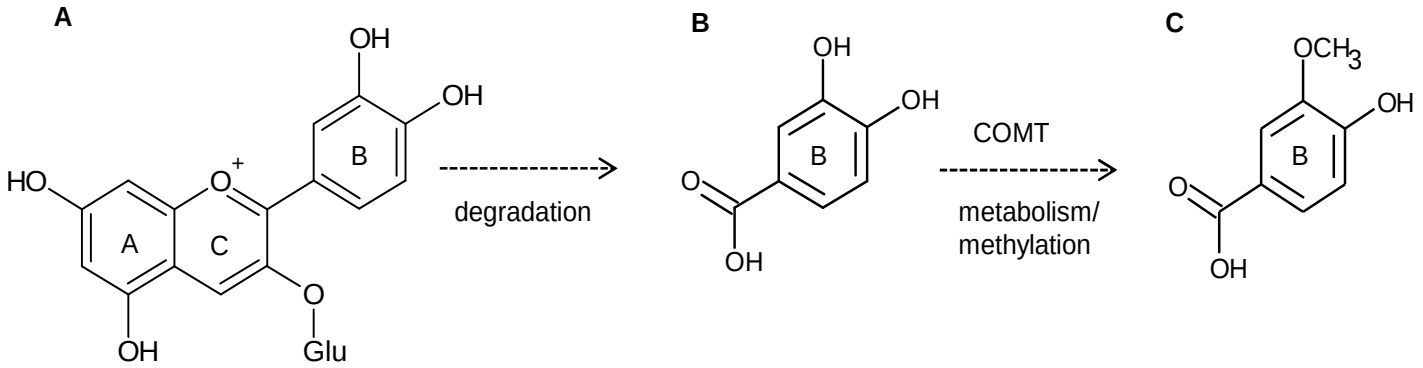
A
OH
OH
HO
O+
B
A
C
O
OH
Glu
degradation
B
OH
OH
O
OH
B
COMT
metabolism/
methylation
C
OCH3
OH
O
OH
B

Figure 2

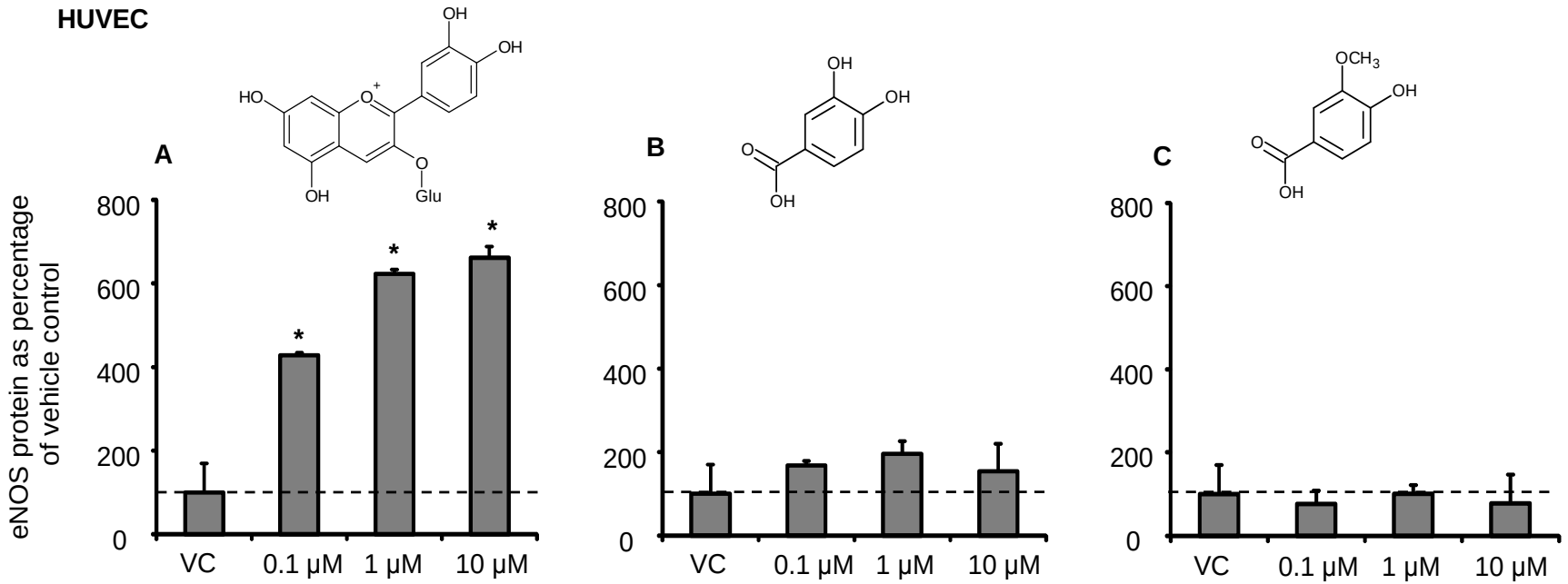
HUVEC
A
B
C
eNOS protein as percentage of vehicle control
800
600
400
200
0
VC
0.1 μM
1 μM
10 μM
*
OH
HO
O
Glu
OCH3

Figure 3

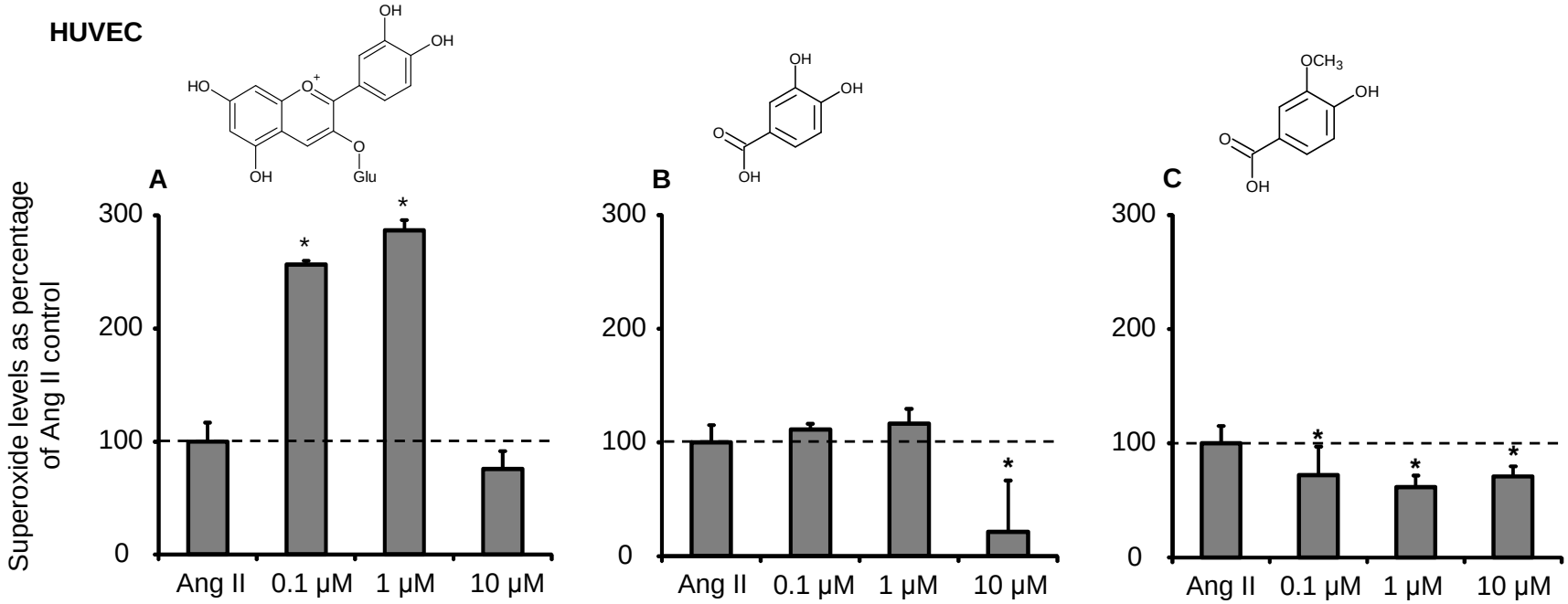
HUVEC
A
B
C
Superoxide levels as percentage of Ang II control
300
200
100
0
Ang II
0.1 μM
1 μM
10 μM
OH
HO
O
Glu
OCH3

Figure 4

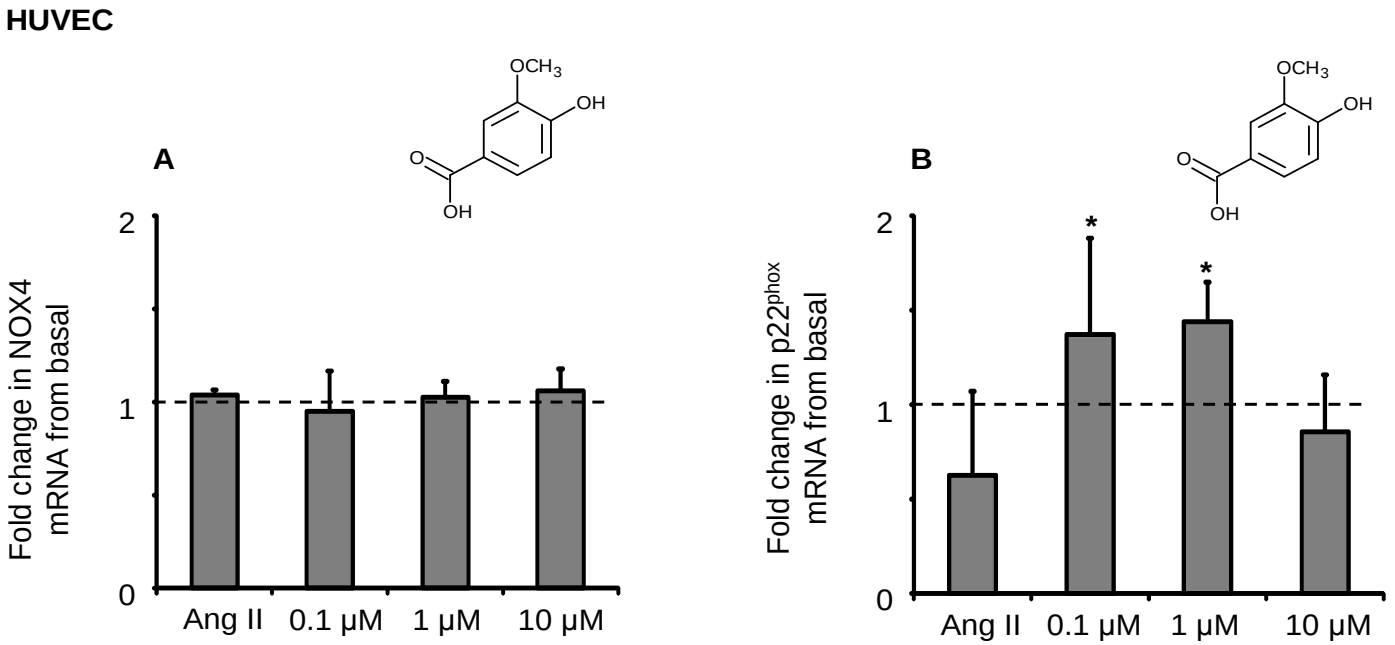
HUVEC
A
B
OCH3
OH
O
OH
Fold change in NOX4 mRNA from basal
Fold change in p22phox mRNA from basal
2
1
0
*
*
Ang II
0.1 μM
1 μM
10 μM

Figure 5

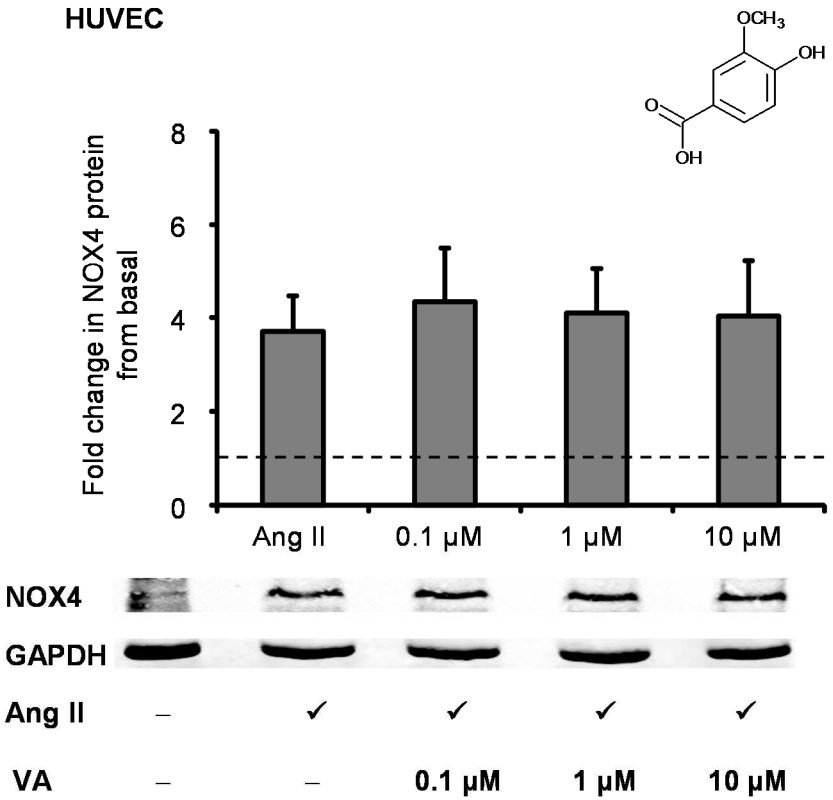
HUVEC
OCH3
OH
O
OH
Fold change in NOX4 protein from basal
8
6
4
2
0
Ang II
0.1 μM
1 μM
10 μM
NOX4
GAPDH
Ang II – ✓ ✓ ✓ ✓
VA – – 0.1 μM 1 μM 10 μM

Figure 6

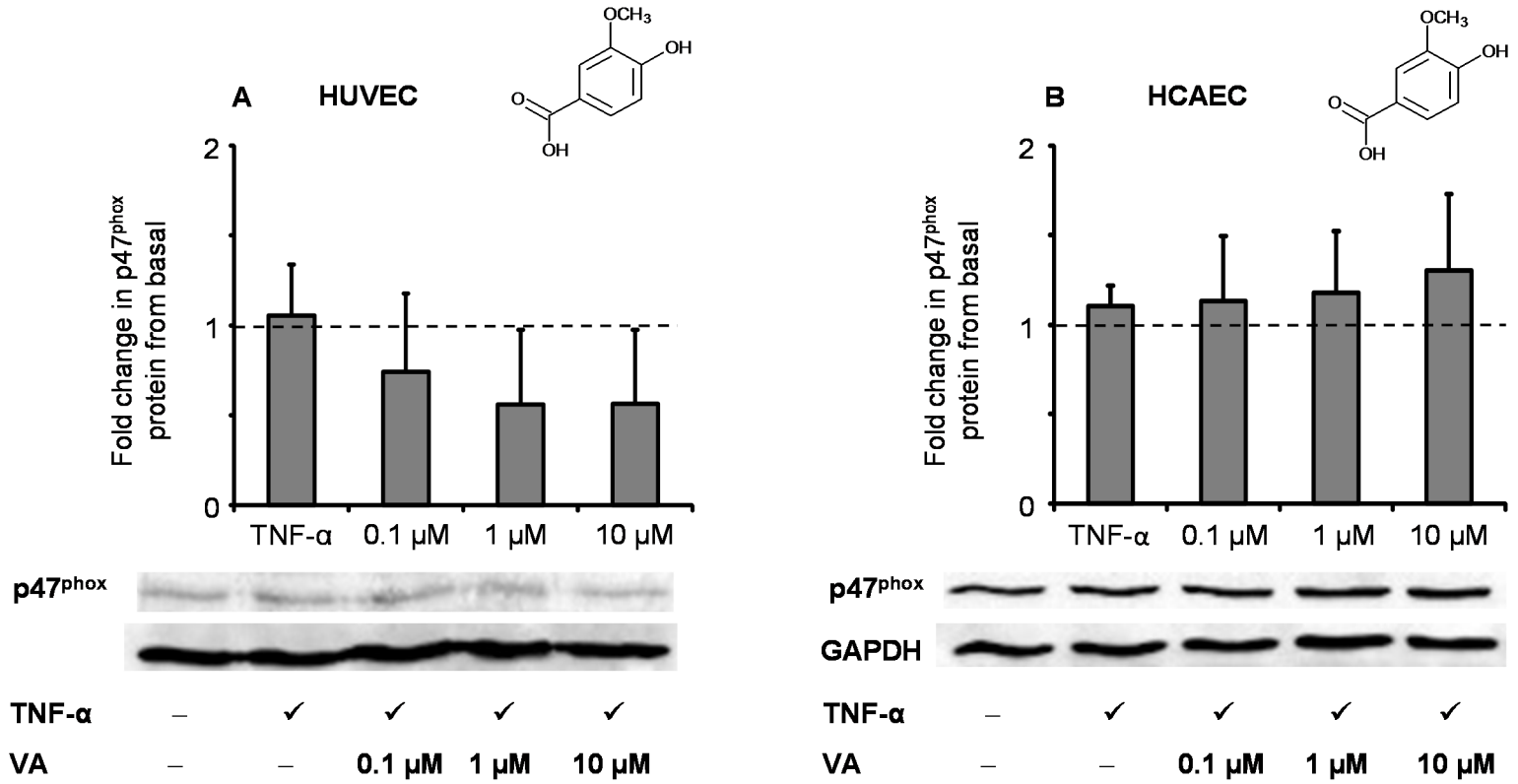
A
HUVEC
OCH3
OH
O
OH
Fold change in p47phox protein from basal
2
1
0
TNF-α
0.1 μM
1 μM
10 μM
p47phox
TNF-α – ✓ ✓ ✓ ✓
VA – – 0.1 μM 1 μM 10 μM
B
HCAEC
OCH3
OH
O
OH
Fold change in p47phox protein from basal
2
1
0
TNF-α
0.1 μM
1 μM
10 μM
p47phox
GAPDH
TNF-α – ✓ ✓ ✓ ✓
VA – – 0.1 μM 1 μM 10 μM

Figure 7

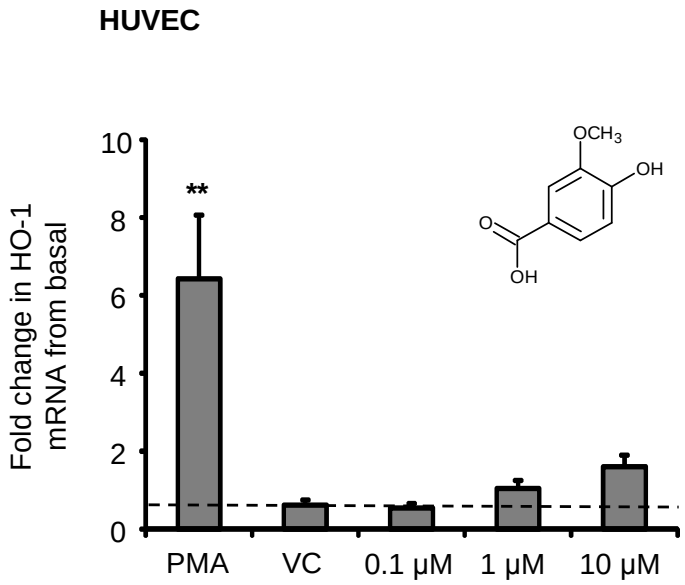
HUVEC
Fold change in HO-1 mRNA from basal
10
8
6
4
2
0
**
PMA
VC
0.1 μM
1 μM
10 μM
OCH3
OH
O
OH

Figure 8

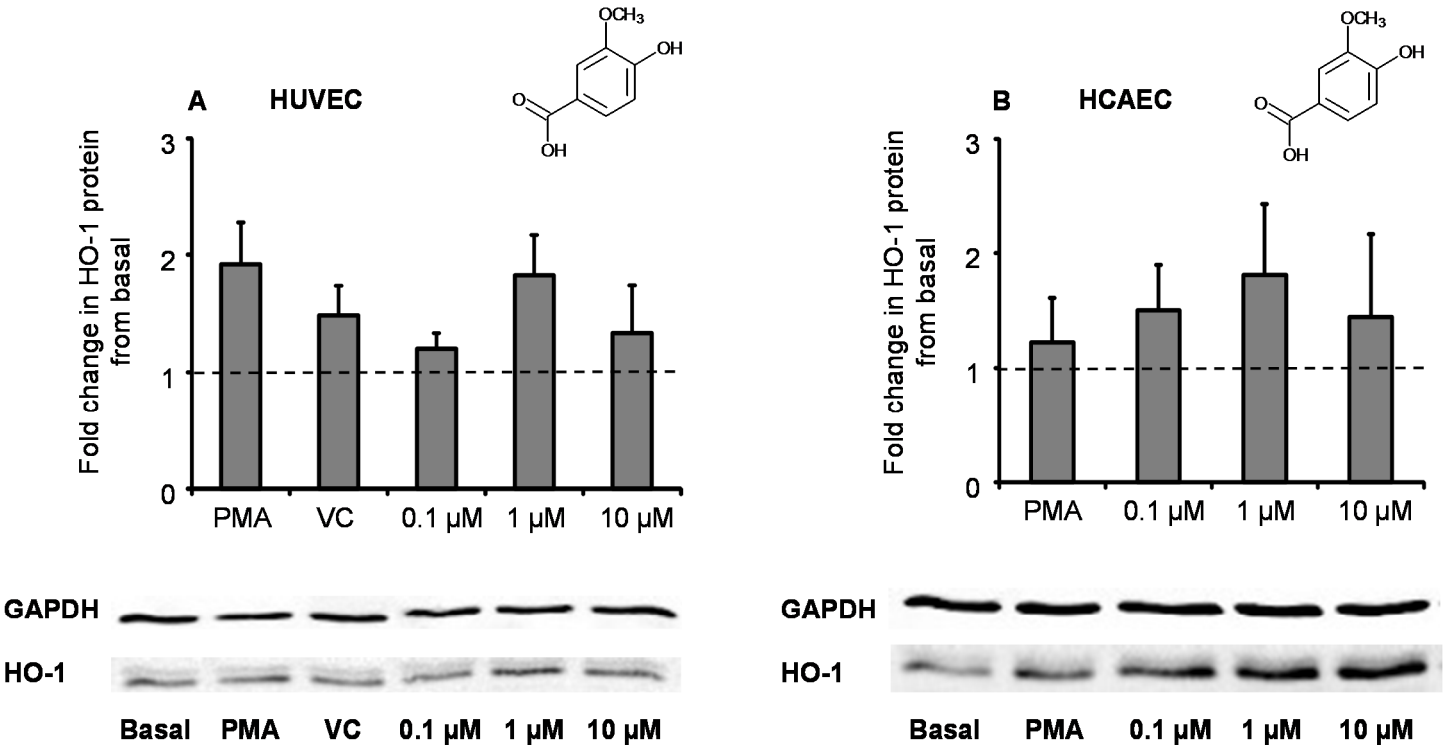
A
HUVEC
OCH3
OH
O
OH
Fold change in HO-1 protein from basal
3
2
1
0
PMA
VC
0.1 μM
1 μM
10 μM
GAPDH
HO-1
Basal
PMA
VC
0.1 μM
1 μM
10 μM
B
HCAEC
OCH3
OH
O
OH
Fold change in HO-1 protein from basal
3
2
1
0
PMA
0.1 μM
1 μM
10 μM
GAPDH
HO-1
Basal
PMA
0.1 μM
1 μM
10 μM

Graphic for Table of Contents only